

Asymmetric bias voltage dependence of the magnetoresistance of Co/Al₂O₃/Co magnetic tunnel junctions: Variation with the barrier oxidation time

Citation for published version (APA):

Oepts, W., Gillies, M. F., Coehoorn, R., Veerdonk, van de, R. J. M., & Jonge, de, W. J. M. (2001). Asymmetric bias voltage dependence of the magnetoresistance of Co/Al₂O₃/Co magnetic tunnel junctions: Variation with the barrier oxidation time. *Journal of Applied Physics*, 89(12), 8038-8045. <https://doi.org/10.1063/1.1375805>

DOI:

[10.1063/1.1375805](https://doi.org/10.1063/1.1375805)

Document status and date:

Published: 01/01/2001

Document Version:

Publisher's PDF, also known as Version of Record (includes final page, issue and volume numbers)

Please check the document version of this publication:

- A submitted manuscript is the version of the article upon submission and before peer-review. There can be important differences between the submitted version and the official published version of record. People interested in the research are advised to contact the author for the final version of the publication, or visit the DOI to the publisher's website.
- The final author version and the galley proof are versions of the publication after peer review.
- The final published version features the final layout of the paper including the volume, issue and page numbers.

[Link to publication](#)

General rights

Copyright and moral rights for the publications made accessible in the public portal are retained by the authors and/or other copyright owners and it is a condition of accessing publications that users recognise and abide by the legal requirements associated with these rights.

- Users may download and print one copy of any publication from the public portal for the purpose of private study or research.
- You may not further distribute the material or use it for any profit-making activity or commercial gain
- You may freely distribute the URL identifying the publication in the public portal.

If the publication is distributed under the terms of Article 25fa of the Dutch Copyright Act, indicated by the "Taverne" license above, please follow below link for the End User Agreement:

www.tue.nl/taverne

Take down policy

If you believe that this document breaches copyright please contact us at:

openaccess@tue.nl

providing details and we will investigate your claim.

Asymmetric bias voltage dependence of the magnetoresistance of Co/Al₂O₃/Co magnetic tunnel junctions: Variation with the barrier oxidation time

W. Oepts^{a)}

Department of Physics and COBRA, Eindhoven University of Technology, 5600 MB Eindhoven, The Netherlands

M. F. Gillies and R. Coehoorn

Philips Research Laboratories, Prof. Holstlaan 4, 5656 AA Eindhoven, The Netherlands

R. J. M. van de Veerdonk^{b)} and W. J. M. de Jonge

Department of Physics and COBRA, Eindhoven University of Technology, 5600 MB Eindhoven, The Netherlands

(Received 23 August 2000; accepted for publication 30 March 2001)

Recently it has been observed that the magnetoresistance (MR) of plasma oxidized exchange biased Co/Al₂O₃/Co tunnel junctions can have a strongly asymmetric bias voltage (V_{bias}) dependence. In this article we report on the dependence of this phenomenon on barrier oxidation time t_{ox} . For junctions based on 1.5 nm Al, t_{ox} was varied from 20 to 120 s. For $t_{\text{ox}} = 20$ s, for which the MR is approximately 20% at $V_{\text{bias}} = 0$, and for $t_{\text{ox}} \geq 90$ s symmetric MR(V_{bias}) curves are found, with the MR decreasing monotonically with $|V_{\text{bias}}|$. A strong asymmetric bias voltage dependence was observed for intermediate oxidation times, which correspond to essentially full oxidation of the Al layer, but almost no formation of stoichiometric CoO at the bottom electrode. Samples with $t_{\text{ox}} = 60$ s show even an asymmetric double peak in MR(V_{bias}). Due to its strength, it has an important consequence for device applications: for a series of junctions with variable t_{ox} the maximum signal voltage (at a fixed current) is not necessarily obtained for junctions which have the largest MR ratio at $V_{\text{bias}} = 0$. © 2001 American Institute of Physics. [DOI: 10.1063/1.1375805]

I. INTRODUCTION

Magnetic tunnel junctions (MTJs) consisting of two ferromagnetic electrodes separated by an insulating barrier show a sizable magnetoresistance (MR) effect when the mutual alignment of the magnetization of the two layers is changed in the presence of an external field.¹⁻³ The effect is the result of spin dependent tunneling, its application for low field magnetoresistive thin film read heads for high density magnetic recording and magnetic random access memory cells is being considered.⁴⁻⁶ The realization of a good tunnel barrier by oxidation of a thin Al layer into Al₂O₃ has formed a major breakthrough.¹ The initial Al thickness in combination with the total oxidation time have a large influence on the final electric properties of the junction and both must be optimized in order to achieve the largest MR ratios.⁷

When applying a magnetic tunnel junction as a sensor element or memory element at a fixed sense current I_{sense} or bias voltage V_{bias} the maximal signal voltage V_{signal} or signal current I_{signal} , respectively, are given by

$$\Delta V_{\text{signal}}^{\text{max}} = \left(\left(\frac{R_0 - R_{\text{sat}}}{R_{\text{sat}}} \right)_{I_{\text{sense}}} \times I_{\text{sense}} \times R_{\text{sat}} \right)_{\text{max}} \quad (1)$$

and

$$\Delta I_{\text{signal}}^{\text{max}} = \left(\left(\frac{R_0 - R_{\text{sat}}}{R_{\text{sat}}} \right)_{V_{\text{bias}}} \times \frac{V_{\text{bias}}}{R_{\text{sat}}} \right)_{\text{max}} \quad (2)$$

with R_0 the zero magnetic field resistance, R_{sat} the resistance at high field, and where the MR ratio ($(R_0 - R_{\text{sat}})/R_{\text{sat}}$) and R_{sat} are taken at the applied sense current or bias voltage, respectively. It is well known that the MR ratio of tunnel junctions decreases with increasing bias voltage.^{1,8} An indication of the size of decrease of the MR with bias voltage is given by the voltage V_{half} at which the MR is half its zero bias value. In the literature values for V_{half} of 500 up to 800 mV are reported for single barrier systems.^{9,10} From Eq. (2) we observe that the largest signal output at constant bias voltage is obtained when the right-hand side of the equation is optimized with respect to the V_{bias} . A large MR at $V_{\text{bias}} = 0$ is not the only issue when high signals are desired, the value of V_{half} must be large as well. This is of importance for future applications utilizing magnetic tunnel junctions. A similar discussion, with I_{half} instead of V_{half} , would apply in the case of operation at a constant sense current [Eq. (1)].

In this article we report on the results of a study on the influence of the plasma oxidation time (t_{ox}) of the barrier on the resistance and magnetoresistance of exchange biased magnetic tunnel junctions. A series of junctions with various oxidation times was fabricated and is characterized by means of electrical transport measurements, magnetoresistance measurements, and investigations of the MR versus applied bias voltage. A key result is that within a certain interval of oxidation time $t_{\text{min}} < t_{\text{ox}} < t_{\text{max}}$ the shape of the MR versus

^{a)}Present Address: Philips Research Laboratories, Prof. Holstlaan 4, 5656 AA Eindhoven, The Netherlands; electronic mail: wouter.oepts@philips.com

^{b)}Present Address: Seagate Research, 2403 Sidney Street, Pittsburgh, PA 15203.

V_{bias} shows a double peak structure. Such a shape is beyond the asymmetric polarity dependences predicted by commonly used models for magnetotransport across asymmetric barriers. The asymmetric bias dependence is shown to give rise to a higher maximum signal voltage than for junctions which have a similar or even higher MR at $V_{\text{bias}}=0$, but which have been oxidized for a time $t_{\text{ox}} < t_{\text{min}}$, and which have a symmetric dependence of the MR. The results of these measurements confirm that the oxidation of the barrier proceeds in four phases.

II. FABRICATION

A series of exchange-biased magnetic tunnel junctions was fabricated with the use of an *in situ* shadow mask system with a cross-bar geometry. The junction electrodes are prepared by dc magnetron sputtering in an ultrahigh vacuum deposition system with a base pressure of 1.3×10^{-7} Pa (1×10^{-9} Torr). The deposition procedure is as follows. First, a 200 μm wide bottom electrode is deposited on a Si substrate with the following structure: 3.5 nm Ta/3.0 nm $\text{Ni}_{80}\text{Fe}_{20}$ /20.0 nm $\text{Fe}_{50}\text{Mn}_{50}$ /2.5 nm $\text{Ni}_{80}\text{Fe}_{20}$ /1.5 nm Co. Then a 1.5 nm Al layer is deposited without mask and subsequently oxidized in a separate chamber ($P_{\text{base}}=2.6 \times 10^{-7}$ Pa) with a glow discharge in an oxygen atmosphere of 9.2 Pa. The glow discharge is ignited from a ring-shaped cathode at a voltage of -1.6 kV with respect to the grounded counter electrode. In one run 24 junctions are fabricated on a wafer, using a shadow mask that was subdivided in four quadrants with each a series of six nominally identical junctions. Six series were fabricated, with the total oxidation time equal to 20, 30, 40, 60, 90, and 120 s. Then, again through a shadow mask, a 200 μm wide top electrode consisting of 4.0 nm Co/10 nm $\text{Ni}_{80}\text{Fe}_{20}$ /3.5 nm Ta is deposited. After deposition, the exchange-biasing direction of the 2.5 nm $\text{Ni}_{80}\text{Fe}_{20}$ /1.5 nm Co layer that is in direct contact with the $\text{Fe}_{50}\text{Mn}_{50}$ layer is defined by heating the junction to 420 K (the blocking temperature of $\text{Fe}_{50}\text{Mn}_{50}$) and slowly cooling in a field of 12 kA/m (150 Oe) parallel to the bottom electrodes. During deposition a field of approximately 16 kA/m is applied in the direction of the electrode stripes, naturally resulting in junctions with a crossed anisotropy. This configuration is preferable for magnetic field sensing devices, as it results in a low coercivity hard-axis magnetization loop for the free (unbiased) electrode layer.

III. COMPOSITION

With the use of Rutherford backscattering spectroscopy (RBS) and elastic recoil detection (ERD) the amount of oxygen incorporated in the Al layer of a series of planar samples has been determined. These samples consist of 20 nm Co/1.5 nm $\text{Al}+t_{\text{ox}}\text{O}_2$ /15 nm Co on Si, with t_{ox} varying from 5 to 600 s. Details of these measurements are described elsewhere.¹¹ Here, we will limit the discussion to the results. In Fig. 1 the amount of O incorporated in the Al obtained by these two techniques, is shown for the samples with varying t_{ox} . Given the (measured) amount of Al atoms in the layer ($10 \times 10^{15} \text{at/cm}^2 \hat{=} 1.5 \text{ nm Al}$) the amount of O needed to form stoichiometric Al_2O_3 is $15 \times 10^{15} \text{at/cm}^2$. This quantity

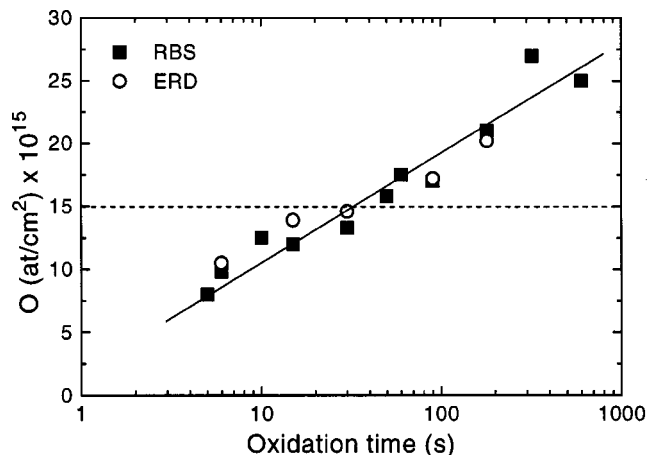


FIG. 1. The O content as a function of the oxidation time as determined via RBS (squares) and ERD (circles). The solid line is a guide to the eye, and the dashed line indicates the amount of oxygen needed for stoichiometric Al_2O_3 . Figure taken from Ref. 11.

is indicated in the figure as a dashed line. The figure shows that after approximately 30 s the amount of oxygen atoms incorporated would be sufficient for the formation of stoichiometric Al_2O_3 . The figure also shows that incorporation of O continues after $t_{\text{ox}}=35$ s. This suggests that for longer t_{ox} the Co bottom layer participates in the oxidation process. We note that these analysis methods yield the Al:O ratio, but cannot reveal a possible variation of the Al:O ratio within the barrier.

A transmission electron microscopy (TEM) study of a multilayer structure, $(\text{Co}/1.5 \text{ nm Al}+t_{\text{ox}})_n$, in which t_{ox} increases with successive repetition, has revealed that the thickness of the oxide layer increases monotonically up to $t_{\text{ox}} \approx 10$ s to 2.2 ± 0.1 nm.¹² This is only slightly larger than the thickness of 1.9 nm that would be expected when 1.5 nm Al is oxidized into unstrained crystalline Al_2O_3 . The actual amorphous oxide is expected to be slightly less dense than crystalline Al_2O_3 , which would explain the difference. The layer thickness increases again for $t_{\text{ox}} \geq 100$ s.

Additional investigations of oxidized planar Al films on top of a Co bottom layer were carried out with *in situ* x-ray photoelectron spectroscopy (XPS).¹³ The spectra show well-separated Al 2*p* core level peaks, corresponding to metallic Al and AlO_x , of which the intensity ratios vary with the composition. The Al-peak intensity has already halved after $t_{\text{ox}}=4$ s, and the peak disappears for $30 \text{ s} < t_{\text{ox}} < 40 \text{ s}$. At $t_{\text{ox}}=40$ s all the Al is oxidized. Unfortunately, the Co and CoO_x 3*p* core level peaks are less well separated, and the sensitivity to these deep lying layers is relatively weak, making an analysis of the oxidation of the top surface of the Co bottom layer less easy. A preliminary analysis suggests that CoO formation starts around 40 s. A more detailed analysis will be published elsewhere.¹³

Another method to investigate the formation of CoO is to perform low temperature magnetization measurements of oxidized planar 1.5 nm Al films on a Co bottom layer. At low temperature CoO is known to be an antiferromagnet, resulting in an exchange biasing of the underlying unoxidized Co layer, for temperatures below the blocking tem-

perature $T_B \approx 280$ K. Magnetization measurements as a function of magnetic field were taken for four samples with $t_{ox} = 20, 40, 80,$ and 250 s, both at $T = 10$ K and room temperature. For $t_{ox} = 20$ s the coercivity of the Co layer did not change upon cooling to $T = 10$ K. However, at $t_{ox} = 40$ s a small increase of the coercivity of the Co layer is already observed, while for longer oxidation times a large exchange biasing is visible. These results indicate that at $t_{ox} \approx 40$ s the formation of CoO is beginning.

These RBS, ERD, TEM, XPS, and magnetization measurements results will be compared in Sec. V with our magnetoresistance measurements in order to correlate the observed MR data with the oxidation process of the Al layer.

IV. RESISTANCE AND MAGNETORESISTANCE

Before presenting the observed asymmetric bias voltage dependence in Figs. 5 and 6, which is the main subject of this article, we first discuss the magnetoresistance at zero bias voltage. Since electrical measurements at exactly zero bias voltage are not possible, we define the MR measured at a V_{bias} below 10 mV as the MR value at $V_{bias} = 0$.

All the junctions fabricated showed a wide plateau in the magnetoresistance, indicating that the antiparallel alignment of the two magnetization directions of the electrodes is reached. The resulting magnetoresistance is well defined, which makes it possible to study the junction magnetoresistance as a function of t_{ox} . As an example we show in Fig. 2(a) the magnetoresistance result at room temperature of a junction with a bottom electrode of 3.5 nm Ta/3.0 nm $Ni_{80}Fe_{20}$ /20.0 nm $Fe_{50}Mn_{50}$ /2.5 nm $Ni_{80}Fe_{20}$ /1.5 nm Co, a barrier consisting of a 40 s oxidized 1.5 nm Al layer, and the top electrode of 4.0 nm Co/10.0 nm $Ni_{80}Fe_{20}$ /3.5 nm Ta. The observed magnetoresistance, defined as $100 \times (R_{AP} - R_P)/R_P$, is 21%. Due to the growth of the junction with a crossed anisotropy configuration, the free layer magnetization is expected to rotate to the hard axis direction when a sufficiently large field is applied parallel to the (exchange-biased) bottom electrode. From the figure it is seen that the free layer magnetization change is in fact the combination of a rotation process (gradual) and domain wall movement processes (sudden), visible as small (reproducible) jumps in the MR curve. The latter can be reduced by decreasing the (4.0 nm) Co layer of the top electrode. In the inset an enlargement of the MR curve is shown, showing that the exchange-biasing field is equal to 17 kA/m (220 Oe). The magnetoresistance curves from the junctions grown in the same run, as well as those oxidized at different oxidation times resembled these curves. The coercivity is observed to be independent of t_{ox} , as is shown in Fig. 2(b). For the junction shown in Fig. 2(a) a coercivity of ~ 1 kA/m is observed for the free layer. A small shift of the MR curve (free layer switches) from zero field is observed. This can be explained by a small ferromagnetic coupling of the Co/ $Ni_{80}Fe_{20}$ top electrode to the exchange-biased bottom electrode. In the case of this junction, the coupling field is 0.6 kA/m (7.5 Oe).

As is shown in Fig. 3(a) the junction resistances varied from 150 Ω (resistance-area product $RA = 6$ M $\Omega \mu m^2$) to 200 k Ω ($RA = 8000$ M $\Omega \mu m^2$), depending on the oxidation

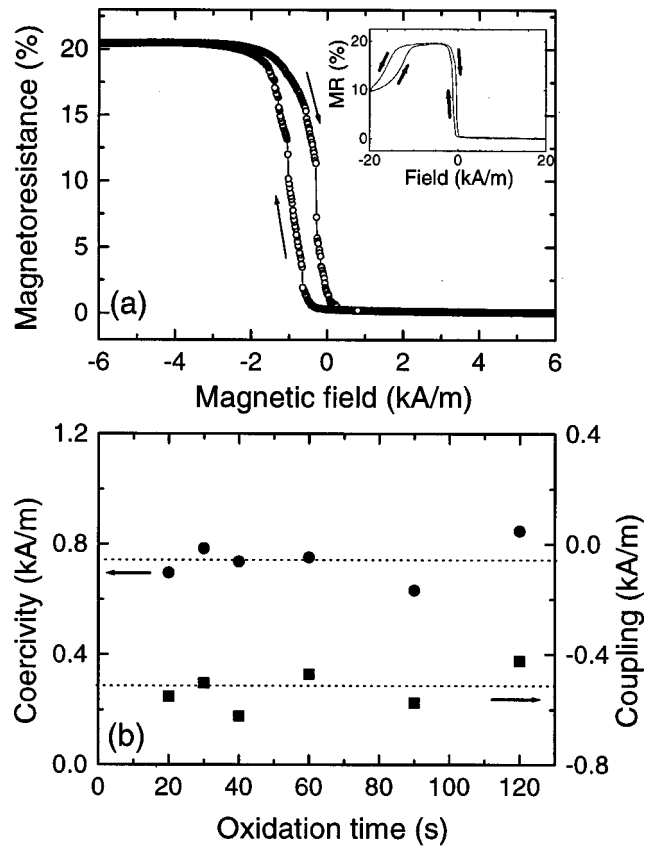


FIG. 2. (a) Magnetoresistance of a Ta/ $Ni_{80}Fe_{20}/Fe_{50}Mn_{50}/Al_2O_3/Ni_{80}Fe_{20}/Co/Ta$ junction, with a barrier consisting of a 40 s oxidized 1.5 nm Al layer. (b) The coercivity and coupling field of the top electrode for the series of junctions as function of the oxidation time.

time. The sheet resistance of the leads is 20 and 30 Ω /square for the top and bottom electrode, respectively, so no current distribution effect on the measured resistance is expected.¹⁴ For the series oxidized for 20, 30, or 40 s the resistances obtained for the 24 junctions fabricated in the same run showed a variation of a factor of two or less. For longer oxidation times the resistances of the junctions in the same run and situated close to each other on the wafer varied only a factor of two or less. However, junctions situated at a larger distance from each other on the wafer could differ a factor of ten in the resistance. These large resistance differences were observed to be systematic in the sense that on each wafer this variation was observed. We return to this issue below. The results presented in Figs. 2 and 3 and discussed below are all taken from a series of six junctions situated close to each other and are believed to have comparable structural properties of the bottom electrodes. The series shown are from a row of junctions which have the lowest junction resistance compared with the other junctions on the wafer, those obtained for the three other quadrants.

Figure 3(a) shows that, initially, the resistance increases logarithmically with oxidation time. For oxidation times above 90 s the increase of the resistance is weaker, on the logarithmic scale used in this figure. Since the tunnel resistance is an exponential function of the barrier thickness, the logarithmic increase of the resistance would be consistent with a linear increase of the barrier thickness as a function of

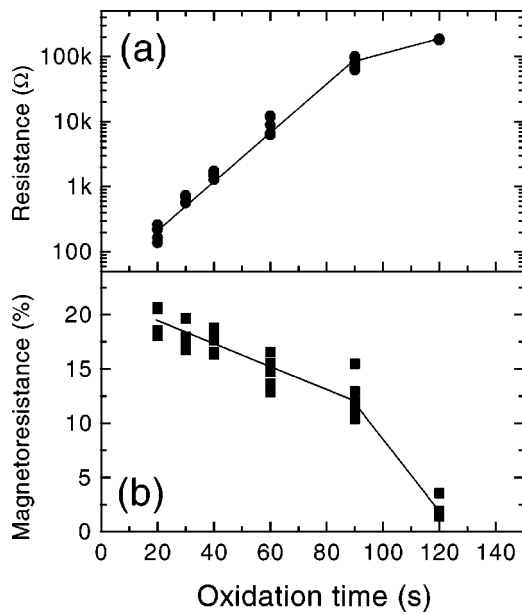


FIG. 3. (a) resistances of the series of junctions (composition see Sec. II) vs increasing oxidation time and (b) magnetoresistance of the same junctions at a very low bias voltage. The straight lines are a guide to the eye. The measurements were carried out at room temperature.

oxidation time. However, if the barrier formed would consist of a laterally uniform layer of stoichiometric Al_2O_3 , this would be inconsistent with the observation of a logarithmic increase of the O content with time as deduced from Fig. 1. A possible complication is that the incorporation of O with oxidation time does not lead immediately to a stoichiometric Al_2O_3 layer but to a thicker substoichiometric AlO_x layer, with a gradient of x across the layer thickness, leading to a different dependence of the resistance with oxidation time. Also, the fact that the tunnel resistance is dominated by the smallest barrier thicknesses and barrier height and therefore does not necessarily represent the mean barrier thickness might contribute to the observed difference.¹⁵ The MR ratio at a low bias voltage is shown in Fig. 3(b). The MR ratio is found to decrease initially almost linearly with oxidation time, and drops above 90 s to nearly zero.

Reproducibility is a strict requirement for carrying out useful studies of the oxidation process, and will be one of the critical factors with regard to the applicability of tunnel junctions. We therefore put much effort in a search for the origin of the observed systematic variation of the resistance across the wafer. The possible difference between the junction stacks at different locations on the wafer has been investigated with scanning Auger microscopy (SAM). In these experiments the junction stack is slowly sputter etched and a depth profile of the junction composition is obtained with Auger electron spectroscopy. In Fig. 4 the depth profile of two junctions ($t_{\text{ox}} = 60$ s) from different wafer regions taken under identical circumstances are shown. The spectra reveal a difference in the width of the Al, O, and Co peaks (the widths of the Fe, Mn, and Ta peaks were identical within the measurement accuracy). This may be interpreted as a difference in roughness of the initial Al layer as well as a difference in intermixing of the Al with the Co bottom electrode.

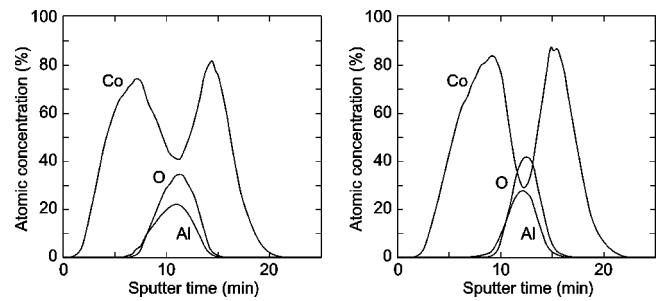


FIG. 4. Two graphs of atomic concentrations of Co, Al, and O as measured with Auger electron spectroscopy during sputter etching of two junction stacks with $t_{\text{ox}} = 60$ s. The junction showing the profile at the left hand side had a lower resistance than the junction of which the profile is shown at the right hand side.

The junctions of the wafer region showing the broadest Al and O peaks, i.e., the largest intermixing, were found to have the lowest resistance values than junctions at the positions elsewhere on the wafer. Recent calculations presented by Bardou¹⁵ have shown that increased roughness and thickness variations of the junction barrier result in lower junction resistances. This may explain the lower resistance values for our junctions with the observed larger intermixing. The underlying cause of this difference in intermixing is most likely an inhomogeneous sputtering process. A detailed study of the fabrication aspects causing these barrier variations is beyond the scope of the work presented in this paper.

For the same junctions the current–voltage (I – V) characteristics were taken. In Fig. 5 the I – V characteristics are shown for four junctions with different oxidation times. In the same figure, on the right-hand side, the differential dI/dV characteristics are given, which were deduced from the measured I – V curves. The positive branch of the I – V characteristic represents the situation of electrons tunneling to the bottom electrode, i.e., the bottom electrode was positively biased. The I – V curves shown in the figure were measured with the magnetization directions of the two electrodes aligned parallel by the presence of an external magnetic field. The graphs with the dI/dV curves show the curves for both the parallel (P) as well as the antiparallel (AP) alignment of the magnetization of the electrodes. The differential dI/dV curve for the junction with $t_{\text{ox}} = 20$ s shows a conductance minimum almost at zero bias voltage. The conductance minimum for the 40 s oxidized junctions is shifted to positive bias indicating an asymmetry in the I – V characteristic. For an oxidation time of 60 s the I – V characteristic is largely asymmetric. The conductance of the 60 s oxidized junction shows a local minimum at zero bias voltage and a global minimum at approximately 200 mV. Asymmetric conductance dependencies on V_{bias} in MTJs have been observed by others,⁹ however the occurrence of two conductance minima in tunnel junctions has, to our knowledge, not been reported before. For the longest oxidation time, 120 s, the I – V curve is symmetric but much more nonlinear compared with the previous curves. The conductance of this junction has a single minimum at zero V_{bias} and is also symmetric around zero. We note that the characteristics of the 90

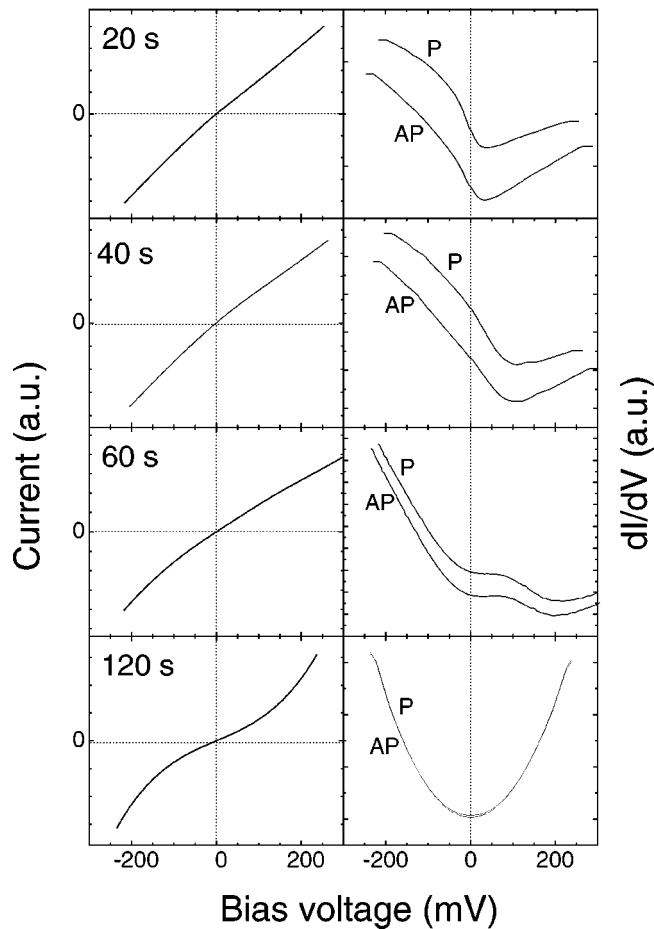


FIG. 5. I - V (left-hand side) and dI/dV (right-hand side) characteristics of four junctions with increasing oxidation time from 20, 40, 60 to 120 s. As the oxidation time increases the I - V curves become increasingly nonlinear. For the dI/dV curves the results for both the AP and P magnetization configuration of the electrodes are shown.

s oxidized junctions were similar to the 120 s oxidized junctions.

In Fig. 6(a) the bias voltage dependencies of the magnetoresistance of the series of tunnel junctions are given. The magnetoresistance is normalized with respect to the value at zero bias. The MR value is obtained within a constant current experiment in which the voltage difference between parallel and antiparallel magnetization alignment is measured. V_{bias} is defined here as the voltage V_P in the situation of parallel alignment. For the junctions with an asymmetric conductance, an asymmetric bias dependence of the MR is observed: the peak value of the MR is not at zero bias, but shifted to the positive side (electrons tunneling to the bottom electrode). The bias dependence of the 60 s oxidized junction shows even two peaks, one at zero bias and an additional peak at $V_{\text{bias}} = 175$ mV. For the 60 s oxidized junctions grown in the same run, this additional peak varied in height and occurred at voltages between 150 and 300 mV. We recall that as was shown in Fig. 5 the conductance of the 60 s oxidized junction also showed two minima for both the parallel and antiparallel magnetization alignment.

A commonly used measure of the MR bias dependence is the voltage at which half of the MR is obtained (V_{half}). In

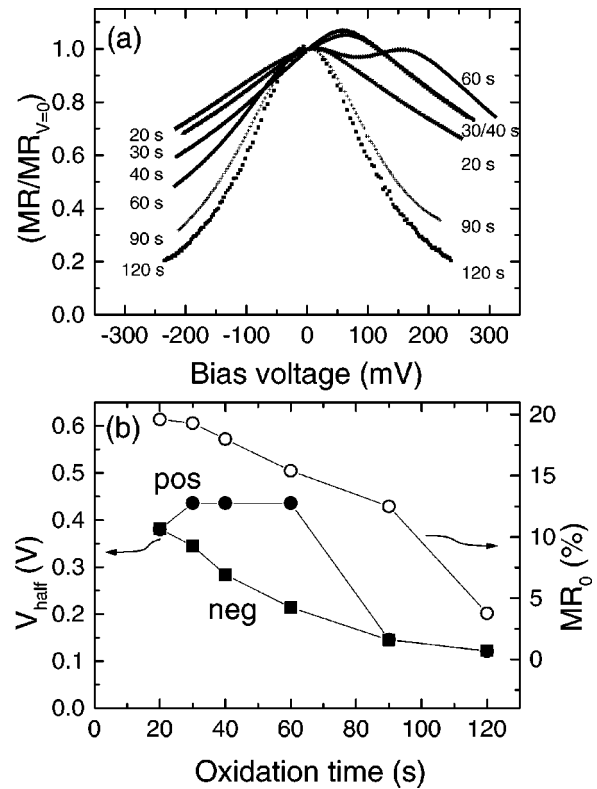


FIG. 6. (a) Voltage bias dependencies of the magnetoresistance of the various junctions, normalized to the value at $V=0$. (b) The voltage V_{half} at which the MR effect is reduced to half its size as a function of oxidation, for the positive and negative polarity of the bias voltage (closed symbols), the open symbols indicate the zero bias value of the MR. The measurements were carried out at room temperature.

Fig. 6(b) V_{half} is given for both polarities. It is found that for negative bias voltages V_{half} decreases with oxidation, while for positive bias voltages V_{half} first increases slightly and drops to the same values as for the negative bias voltages for oxidation times above 60 s. We note that our measured values of V_{half} (above 0.4 V) are comparable to what is presently reported in the literature for plasma oxidized single barrier systems (see for instance the overview table in Ref. 9). The asymmetry introduces much larger (V_{half}) values at positive bias and the change in the voltage $\Delta V = V_{AP} - V_P$ at constant current is thus larger for positively biased junctions. For completeness the near zero bias value of the MR of these junctions is also indicated in Fig. 6(b).

We remark that although the largest value of V_{half} is found for $t_{\text{ox}} = 60$ s and a positive V_{bias} , the largest output signal is obtained for shorter oxidized junctions. This can be seen from Fig. 7, which shows the voltage difference $V_{AP} - V_P$ that arises in a constant-current experiment upon switching the electrode magnetizations from antiparallel to parallel, as a function of V_P for the 20–60 s oxidized junctions. The 40 s oxidized junction shows the largest voltage change, corresponding to $\Delta V \approx 42$ mV at $V_P = 400$ mV. The highest voltage output is always obtained when the junctions are biased positively, which is due to the shift of the peak in the MR bias dependence. These considerations are of importance when the magnetic tunnel junctions are used in an application where a high output is desired.

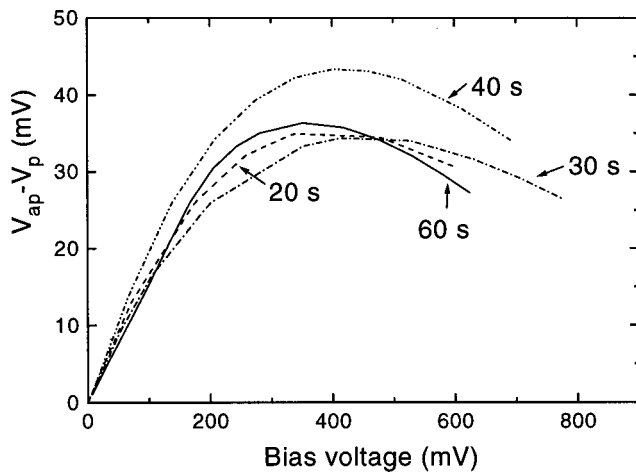


FIG. 7. Resulting voltage difference in a constant-current experiment when the junction electrodes are switched between antiparallel and parallel alignment for junctions with oxidation times 20–60 s. The bias voltage given is equal to V_p .

V. ANALYSIS

The I – V curves of symmetric and asymmetric tunnel junctions can be analyzed by fitting the data to the models of electron tunneling formulated by Simmons¹⁶ and Brinkman,¹⁷ respectively. From these fits the barrier thickness d , and the average height $\bar{\phi}$ are obtained, and, if present, the barrier asymmetry $\Delta\phi$. The asymmetric barrier model of Brinkman would be more appropriate for our 30–60 s oxidized junctions with an asymmetric conductance and magnetoresistance. With this model the I – V curves of the 20 and 30 s oxidized junctions could be fitted, resulting in a barrier asymmetry of 0.4 and 0.8 eV, respectively, with the highest barrier at the interface between the bottom electrode and the oxide. For the 40 and 60 s oxidized layers a consistent fit was not obtained. For the 40 s oxidized junction this may be the result of the asymmetry $\Delta\phi$ being larger than the mean barrier height $\bar{\phi}$, for which the Brinkman model does not give a good approximation. For the 60 s oxidized junction we recall that the conductance showed two minima, a phenomenon that the Brinkman model cannot account for. The Simmons fits of the I – V curves of the two longer oxidized junctions of 90 and 120 s resulted in good fits, with $d=2.6$ and 3.1 nm and $\phi=0.9$ and 0.7 eV, respectively.

The double peak structure of the MR bias dependence for an asymmetric barrier has not been observed before. The dependence of the MR on the voltage bias is an intrinsic property of magnetic tunnel junctions. However, the origin of the MR bias dependence itself is not yet understood perfectly. For symmetric junctions the effect has been related to: excitations of magnons^{18,19} or phonons,¹⁸ inelastic tunneling processes via defects,^{18,20} electron interactions at the electrode–barrier interface,²¹ and the influence of the electric field on the barrier shape (and on the spin dependent transmission coefficients).^{18,22,23}

The latter explanation, which was supported by model calculations of the bias dependence by assuming free electron like electrode metals, can be extended to the case of an asymmetric barrier.^{22,23} We have performed such calcula-

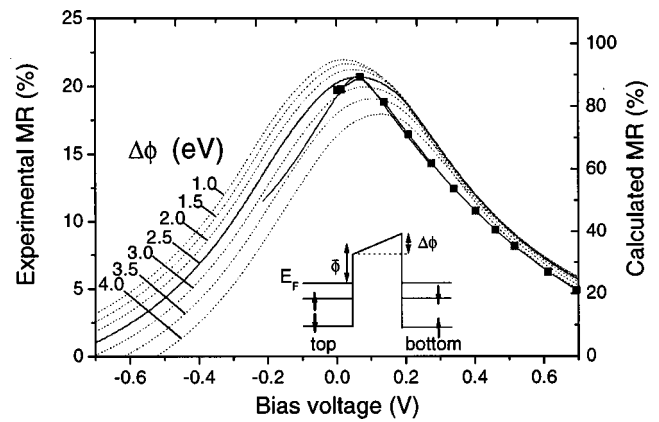


FIG. 8. The asymmetric bias dependence of a 40 s oxidized junction (squares with solid line), compared with the results of free electron calculations. The calculations are carried out for various barrier asymmetries. It is found that an asymmetry of 2.5 eV (indicated as a solid line) resembles the experimental observed bias dependence asymmetry reasonably well. The inset shows a schematical drawing of the potential landscape used in the calculations.

tions assuming for the ferromagnetic electrodes an internal potential (with respect to the Fermi level) equal to -1.1 eV and -0.2 eV for majority and minority spin electrons respectively, a mean barrier height $\bar{\phi}$ of 2.5 eV and a barrier thickness of 1.5 nm. We note that this model and these parameters are merely an assumption and will not exactly describe our electrodes and barrier. The results must be interpreted only as a first indication of the effect of the asymmetry of the potential barrier asymmetry of the MR versus bias voltage. The barrier asymmetry $\Delta\phi$ is defined as the difference in barrier height between the bottom and top electrode: $\Delta\phi = \phi_{\text{bottom}} - \phi_{\text{top}}$. The definition of positive voltage is taken as in the previous section, i.e., positive voltage means a positive biased bottom electrode. In Fig. 8 the results of these calculations are given for various barrier asymmetries. For a barrier asymmetry of 2.5 eV (highest barrier on the bottom electrode side) we find for the maximum of the MR(V_{bias}) curve to a shift to +70 mV, approximately the same as found experimentally at $t_{\text{ox}}=40$ s (see Fig. 8), and also with the same polarity. This model could explain the observed asymmetric bias dependence found by Sato *et al.*⁹ Annealing at 275 °C of junctions with a rf plasma oxidized Al layer as a barrier resulted in a shift of the MR bias dependence curve with +70 mV. Although the detailed mechanism of this shift is unclear, the authors consider the Co–Al interdiffusion and change in bandstructure as a possible cause. However, such a model cannot explain the occurrence of a double peak in the MR(V_{bias}), as observed for $t_{\text{ox}}=60$ s. Moreover, it is difficult to give a physical justification for the extremely large barrier asymmetry required to obtain the observed shift for $t_{\text{ox}}=40$ s.

A possible explanation of the double peak would be in terms of a model of the energy and spin dependent electronic structure of the relevant states at the interface between the bottom electrode and the oxide layer. Recent results obtained for asymmetric junctions, with an additional thin nonmagnetic layer next to the Al_2O_3 barrier²⁴ or the use of a composite $\text{Ta}_2\text{O}_5/\text{Al}_2\text{O}_3$ barrier²⁵ show that for asymmetric bar-

TABLE I. Overview of observations made with several techniques of the oxidation of a 1.5 nm Al layer on a Co bottom electrode during the third stage (10–90 s of plasma oxidation). MR and MH indicate the magnetoresistance and magnetization measurements, respectively and $Z(\omega)$ the ac impedance measurements.

Time (s)	Measurement technique	Observation
8–10	TEM	oxygen is incorporated across full Al layer thickness
30	MR	magnetoresistance curve develops an asymmetry
35	RBS/ERD	oxygen content corresponds to stoichiometric Al_2O_3
40	MH	start of oxidation of the Co bottom electrode
40	$Z(\omega)$	a second dielectric component contributes to the impedance
50	$Z(\omega)$	a third dielectric component contributes to the impedance
60	XPS	oxidation of Al completed
60	MR	asymmetry of MR curves, with a very large second peak
90	MR	asymmetry has disappeared
90	$Z(\omega)$	a fourth dielectric component contributes to the impedance
90	TEM	oxidation front starts to move forward again

riers asymmetric bias dependences may indeed occur. In Ref. 25 the observed asymmetric bias dependence has been related to the different energy dependences of the polarization of the effective density of states at both interfaces. We cannot exclude interpretations of our results in terms of such a model. However, we have strong indications that within the range of oxidation times within which the double peak is observed the bottom electrode interface is structurally and compositionally quite inhomogeneous. Therefore, we will not further attempt to attribute the double peak to a structurally ideal interface but rather give an analysis of the available experimental data on the interface structure. This is the subject of the remainder of this section.

In Sec. III we discussed the results of a wide range of analysis methods to characterize the oxidation process of a 1.5 nm Al layer. In Table I the results are summarized in terms of increasing oxidation time. We have now also incorporated the results of the magnetoresistance and magnetization measurements. Also included are the results obtained with ac impedance [$Z(\omega)$] measurements.¹² Modeling of the measured (complex) impedance curves resulted in a description of the tunnel barrier as a combination of several RC circuits in series: one for the thinnest oxide layer (short oxidation times) up to four for the thickest oxide films ($t_{\text{ox}} = 120$ s). The table gives the oxidation times at which in the equivalent circuit description of the ac impedance an additional RC circuit (“dielectric component”) is required. In Ref. 26 the experimental results (except magnetoresistance) have been discussed and the development of the composition with increasing oxidation time was subdivided into four steps (stages): an initial (first) stage at $t_{\text{ox}} = 0$ s (thermal oxidation before, at $t_{\text{ox}} = 0$ s, the plasma is ignited) and three stages of plasma oxidation. Immediately after ignition of the oxygen plasma, during the second stage, only the Al layer is gradually oxidized. During the third stage the O content in the Al layer increases while the AlO_x layer thickness remains constant. At some points the Al is already oxidized to Al_2O_3 and at these points the oxide/metal bottom electrode interface consists of $\text{Al}_2\text{O}_3/\text{Co}$ and $\text{Al}_2\text{O}_3/\text{CoO}/\text{Co}$ regions. Finally, during the fourth stage, atoms of the bottom electrode at the interface participate in the oxidation process.

The second oxidation stage (i.e., the first plasma oxidation stage) ends when the oxygen is incorporated across the entire Al thickness. This moment can be deduced from the results from TEM experiments, and is reached after an oxidation time of ~ 10 s. Experiments on junctions that were oxidized with $t_{\text{ox}} < 10$ s could not be done due to the occurrence of an inhomogeneous current distribution.¹⁴ The resistance of 20 s oxidized junctions is only ~ 5 times the sheet resistance, and shorter oxidation times will certainly result in resistances of the order of the sheet resistance of the contact leads. The MR ratio during the first and second stage is expected to gradually increase due to the decrease of the amount of metallic Al in the barrier. Others have indeed observed that the MR is lower for junctions with unoxidized Al left over in the barrier.⁷ We do not observe an initial increase of the magnetoresistance for short oxidation times, indicating that for $t_{\text{ox}} \geq 20$ s not much metallic Al is present. This indicates that the second oxidation stage has ended before $t_{\text{ox}} = 20$ s, which is consistent with the TEM results.

During the third stage the Al:O ratio increases, while the barrier thickness remains almost constant. XPS and RBS/ERD measurements show that at $t_{\text{ox}} = 30\text{--}35$ s the overall Al:O ratio corresponds to Al_2O_3 . Earlier, after $t_{\text{ox}} \approx 20\text{--}25$ s, the barrier becomes asymmetric and an MR bias voltage dependence with a maximum shifted from zero or with a double peak structure is obtained. The barrier asymmetry ends at some time between 60 and 90 s oxidation. The third stage ends at $t_{\text{ox}} = 90$ s when the oxidation front starts to move forward again. A first possible reason for the observed asymmetry and double peak structure of the MR versus the bias voltage could therefore be that different interface structures at the bottom electrode at different (widely separated) parts of the sample are present. For instance, one type of interface region may lead to a symmetric MR bias dependence, while a second type gives rise to an asymmetric MR bias dependence with a shift of the maximum MR to positive V_{bias} . Superposition of these two regions may lead to a bias dependence with two peaks, which is indeed observed in Fig. 6 (double peak structure around 60 s). The presence of $\text{Al}_2\text{O}_3/\text{Co}$ type, $\text{Al}_2\text{O}_3/\text{Al}$ type, and $\text{Al}_2\text{O}_3/\text{CoO}$ type interface regions could play a crucial role in determining the

asymmetry of the $I-V$ and MR bias dependence curves. The barrier height at the $\text{Al}_2\text{O}_3/\text{Co}$ interface is expected to be higher than that of $\text{Al}_2\text{O}_3/\text{Al}$ or CoO/Co , and the apparent barrier height may even be enhanced when roughness is present at this interface.²⁷ A second possible explanation for the observed asymmetric barrier is the existence of a lateral variation on a scale smaller than the barrier thickness of the oxygen content in the barrier or of a lateral variation of the concentration of metal ions (e.g., Al^{3+} and Co^{2+}) in the barrier. In this case the equipotential planes in the barrier are not parallel and thus simple models of the tunnel current (such as the Simmons and Brinkman model) do not hold. As far as we know no models beyond these pseudo-one dimensional models are available.

During the fourth stage at all lateral positions the Co bottom electrode participates in the oxidation process and a CoO layer is formed. At room temperature CoO is a paramagnet within which spin-flip scattering can take place, leading to a further decrease of the magnetoresistance.⁷

The possibility of the plasma oxidation of Al being divided into two steps (stage 2 and 3) has recently been put forward by LeClair *et al.*²⁸ An XPS study of samples with varying Al thicknesses and oxidized for 100 and 200 s, revealed that for both oxidation times the vanishing of the metallic Al $2p$ peak occurs at the same thickness. This is explained by an initial rapid oxidation of Al, for instance via grain boundaries, while at longer times the Al is further oxidized to Al_2O_3 . This observation agrees with the results of our study. A quantitative comparison between both studies cannot be carried out since the oxidation conditions (e.g., geometry, oxygen pressure) for both series of samples differ.

VI. CONCLUSIONS

A series of exchange biased tunnel junctions was prepared with a varying plasma oxidation time. The resulting junctions were characterized by means of transport and magnetoresistance measurements. For junctions oxidized up to 40 s we find MR ratios of 20% combined with a large, but polarity dependent, V_{half} up to 430 mV. For the 30, 40, and 60 s oxidized junctions the $I-V$ and dI/dV characteristics are asymmetric, which resulted in an asymmetric MR bias dependence. For Al_2O_3 based magnetic tunnel junctions such large asymmetric bias dependencies have not been reported so far. For positive V_{bias} the signal voltage V_s , is higher than for negative V_{bias} . As a result of the asymmetric MR bias dependence, the junction with the highest V_s did not have the highest initial MR. The results of these experiments have been described in terms of an oxidation process of the junction that takes place in four stages. The asymmetric $I-V$ characteristics and at $t_{\text{ox}} = 60$ s even a double peak in the bias voltage dependences are observed in the third stage of the oxidation process, from $10 \text{ s} \leq t_{\text{ox}} \leq 90 \text{ s}$, within which oxidation proceeds without an increase of the barrier thickness as observed from TEM. The asymmetry and double peak are

likely to be related to a mesoscopic- or microscopic-scale lateral variation of the composition and structure near the bottom electrode interface induced during deposition (Fig. 4), but activated after >20 s oxidation (Figs. 1 and 6). However, an alternative explanation in terms of an energy dependent electronic structure and effective polarization of the unoccupied states of the bottom electrode cannot be disregarded.

ACKNOWLEDGMENTS

The authors gratefully acknowledge A. E. T. Kuiper for discussions, S. Toussaint for SAM analysis, and M. Maoliyakefu for magnetization measurements. M. van Kampen and A. A. Smits are acknowledged for their contributions to the calculations.

- ¹J. S. Moodera, L. R. Kinder, T. M. Wong, and R. Meservey, *Phys. Rev. Lett.* **74**, 3273 (1995).
- ²T. Miyazaki and N. Tezuka, *J. Magn. Magn. Mater.* **151**, 403 (1995).
- ³W. J. Gallagher *et al.*, *J. Appl. Phys.* **81**, 3741 (1997).
- ⁴H. Tsuge and T. Mitsuzuka, *Appl. Phys. Lett.* **71**, 3296 (1997).
- ⁵J. M. Daughton, *J. Appl. Phys.* **81**, 3758 (1997).
- ⁶S. Gider, B.-U. Runge, A. C. Marley, and S. P. P. Parkin, *Science* **281**, 3288 (1998).
- ⁷J. S. Moodera, E. F. Gallagher, K. Robinson, and J. Nowak, *Appl. Phys. Lett.* **70**, 3050 (1997).
- ⁸Y. Lu, X. W. Li, G. Xiao, R. A. Altman, W. J. Gallagher, A. C. Marley, K. P. Roche, and S. P. P. Parkin, *J. Appl. Phys.* **83**, 6515 (1998).
- ⁹M. Sato, H. Kikuchi, and K. Kobayashi, *IEEE Trans. Magn.* **35**, 2946 (1999).
- ¹⁰H. Boeve, E. Girgis, J. Schelten, J. D. Boeck, and G. Borghs, *Appl. Phys. Lett.* **76**, 1048 (2000).
- ¹¹M. F. Gillies, W. Oepts, A. E. T. Kuiper, R. Coehoorn, Y. Tamminga, J. H. M. Snijders, and W. M. A. Bik, *IEEE Trans. Magn.* **35**, 2991 (1999).
- ¹²M. F. Gillies, A. E. T. Kuiper, R. Coehoorn, and J. J. T. M. Donkers, *J. Appl. Phys.* **88**, 429 (2000).
- ¹³V. Kottler, M. F. Gillies, and A. E. T. Kuiper, *J. Appl. Phys.* **89**, 3301 (2001).
- ¹⁴R. J. M. van de Veerdonk, J. Nowak, R. Meservey, J. S. Moodera, and W. J. M. de Jonge, *Appl. Phys. Lett.* **71**, 2839 (1997).
- ¹⁵F. Bardou, *Europhys. Lett.* **39**, 239 (1997).
- ¹⁶J. G. Simmons, *J. Appl. Phys.* **34**, 1793 (1963).
- ¹⁷W. F. Brinkman, R. C. Dynes, and J. M. Rowell, *J. Appl. Phys.* **41**, 1915 (1970).
- ¹⁸A. M. Bratkovsky, *Appl. Phys. Lett.* **72**, 2334 (1998).
- ¹⁹S. Zhang, P. M. Levy, A. C. Marley, and S. P. P. Parkin, *Phys. Rev. Lett.* **79**, 3744 (1997).
- ²⁰J. Zhang and R. M. White, *J. Appl. Phys.* **83**, 6512 (1998).
- ²¹S. T. Chui, *Phys. Rev. B* **55**, 5600 (1997).
- ²²X. Zhang, B.-Z. Li, G. Sun, and F.-C. Pu, *Phys. Rev. B* **56**, 5484 (1997).
- ²³M. van Kampen, R. J. M. van de Veerdonk, and A. A. Smits, unpublished results.
- ²⁴J. S. Moodera, J. Nowak, L. R. Kinder, P. M. Tedrow, R. J. M. van de Veerdonk, A. A. Smits, M. van Kampen, and H. J. M. Swagten, *Phys. Rev. Lett.* **85**, 3029 (1999).
- ²⁵M. Sharma, S. X. Wang, and J. H. Nickel, *Phys. Rev. Lett.* **82**, 616 (1999).
- ²⁶A. E. T. Kuiper, M. F. Gillies, V. Kottler, G. 't Hooft, G. van Berkum, C. van der Marel, Y. Tamminga, and J. H. M. Snijders, *J. Appl. Phys.* **89**, 1965 (2001).
- ²⁷W. Oepts, Ph.D. thesis, Eindhoven University of Technology, Department of Physics, Eindhoven, The Netherlands, 1999.
- ²⁸P. LeClair, J. Kohlepp, A. Smits, H. Swagten, B. Koopmans, and W. de Jonge, *Appl. Phys. Lett.* **87**, 6070 (2000).